Earth Planets Space, **61**, 973–981, 2009

Co-seismic EM signals in magnetotelluric measurement—a case study during Bhuj earthquake (26th January 2001), India

K. K. Abdul Azeez, C. Manoj, K. Veeraswamy, and T. Harinarayana*

National Geophysical Research Institute, Council of Scientific & Industrial Research, Hyderabad, PIN 500 007, India

(Received December 29, 2006; Revised July 16, 2008; Accepted May 7, 2009; Online published October 19, 2009)

Significant changes in amplitude and frequency characteristics were observed in the magnetotelluric (MT) time series recorded during Bhuj earthquake ($\sim$7.6 M_w), at a site $\sim$350 km from the epicenter. The telluric and magnetic signals recorded in the frequency range (10^{-1}–10^{1} Hz) of MT spectrum show considerable variations in their spectral characteristics during the earthquake event compared to the data recorded before and after the earthquake. The spectral analysis brings out sharp changes in amplitude of low-frequency signals during the earthquake as compared to the typical flat spectrum observed before and after the earthquake. The wavelet analysis of the electric and magnetic field data reveals two different spectral regimes; (1) the flat spectrum related to the natural MT signals, and (2) localized, high amplitude signals (in time and frequency) related to the onset of main shock. Three more high amplitude events are noted in the wavelet spectrum, after the main shock event, and can be speculated to be associated with the after-shock events. The MT impedance estimates clearly show scattered apparent resistivity and phase values during the earthquake suggesting that the high amplitude electric and magnetic signals were not related by an MT transfer function. The MT impedance estimates made before and after the earthquake are strikingly normal and smooth. The Pearson's correlation coefficients between the orthogonal electric and magnetic fields show a drastic drop for the data measured during earthquake, while the MT fields recorded before and after the earthquake are well correlated. The observed MT signals during the seismic activity do not show any external geomagnetic origin and may be attributed to co-seismic EM phenomena. The probable mechanisms responsible for the co-seismic EM phenomena could be electro-kinetic and seismic dynamo effects.

Key words: Co-seismic, electromagnetic, earthquake, Bhuj.

1. Introduction

Anomalous electromagnetic signals associated with seismic activity has been reported extensively over a wide frequency range of few MHz to ultra low frequency (Hattori *et al*., 2006 and references therein). These electromagnetic signals may be precursory (prior to earthquake) or co-seismic (coincident with earthquakes). The observation and analysis of these earthquake associated EM phenomena is being used for seismic prediction and to understand the subsurface physical mechanism related with the EM phenomenon. EM signals associated with seismic activities have been studied using ground and satellite based observations. The ground based observations include the monitoring of electric field variations (e.g. Nagao *et al*., 2000; Fujinawa *et al*., 2001; Enomoto *et al*., 2006; Singh *et al*., 2006; Widarto *et al*., 2009) or magnetic fields (e.g. Nagao *et al*., 2002; Hattori *et al*., 2006) or in combination (e.g. Honkura *et al*., 2000, 2004; Zlotnicki *et al*., 2001; Karakelian *et al*., 2002). More recently, ground based EM studies combined with satellite EM monitoring approach is used to study the EM phenomena related to volcanic eruptions and earthquakes (Zlotnicki *et al*., 2006).

The Kutch region, being considered as a part of the stable continental region, experienced the most disastrous earthquake in India's recent history on 26th January 2001 earthquake. The epicenter location of this 7.6 M_w earthquake was located at 23.36°N, 70.34°E, 60 km east of Bhuj and estimated a focal depth of 22 km by U.S. Geological Survey (USGS). The event, with origin time of 03:16:40.7 UT, caused a death of at least 20,000 people and injured more than 200,000. It destroyed about 400,000 houses and twice as many damaged. This devastating 26th January 2001 Bhuj earthquake provided an accidental opportunity to observe anomalous EM signals in magnetotelluric (MT) measurement conducted at a location $\sim$350 km away from the epicenter (Fig. 1). In this study, we discuss the analysis of the MT time series acquired prior, during and after the 7.6 M_w Bhuj earthquake.

2. Magnetotelluric (MT) Observations

The observation point (MT recording site) is located in the Deccan volcanic province of western India, just south to the Narmada river (Fig. 1). The site was relatively free from cultural electromagnetic noises. The data were acquired as a part of an MT campaign for hydrocarbon exploration in Cambay and Narmada basins (Harinarayana *et al*., 2004). Five component MT time series (three orthog-

*Presently at Beaureau of Economic Geology, University of Texas, USA.

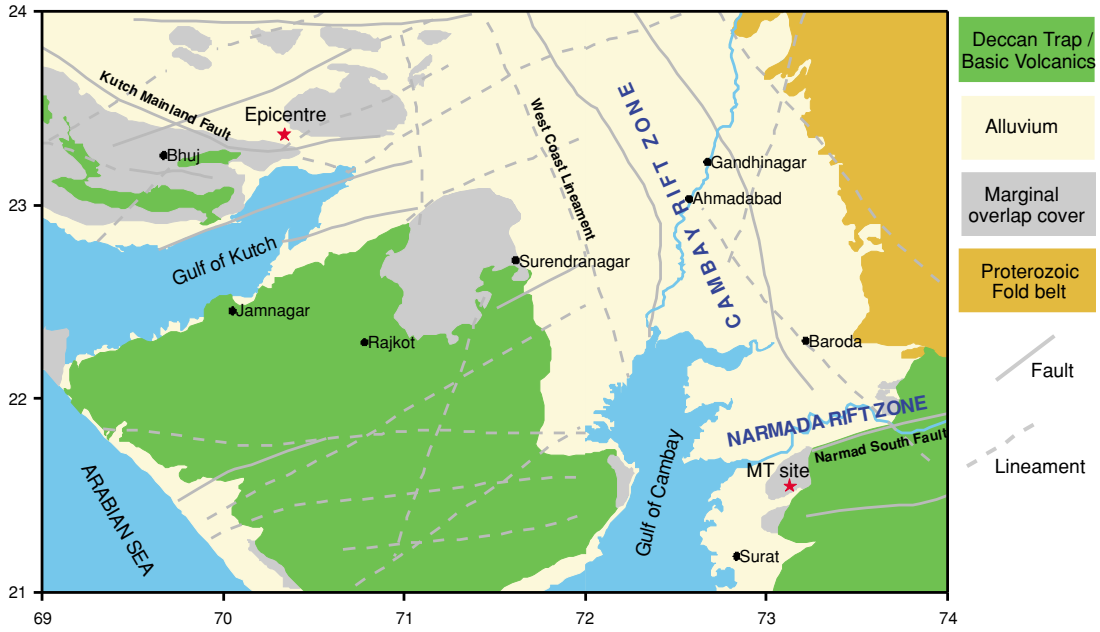

Fig. 1. Location of Bhuj Earthquake (26th January, 2001) epicenter and MT observation site shown over the geological subdivisions and tectonic features in western India (after GSI, 2000).

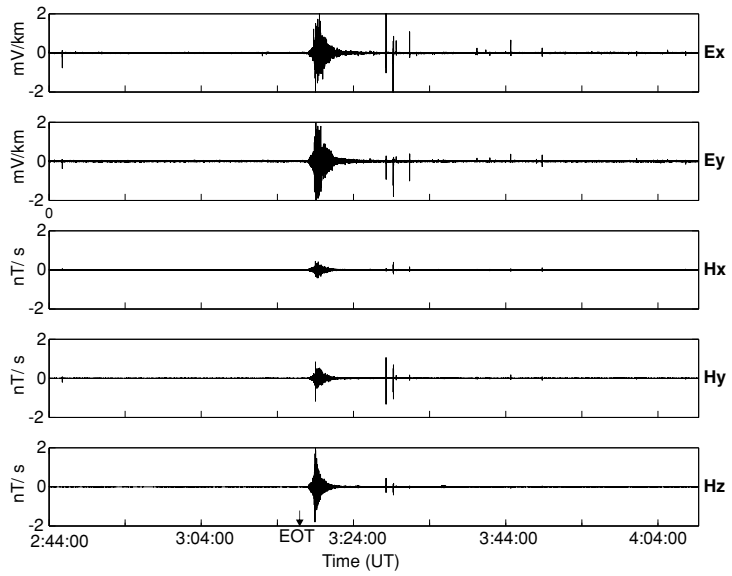

Fig. 2. The plot of MT time series data measured in the 10^{-1}–10^{1} Hz frequency range. The recording started at 2:44:00 UT and continued up to 4:09:00 UT on 26th January 2006. The origin time of Bhuj earthquake is marked as EOT. Note the increase in signal amplitudes in the electric as well as magnetic fields.

onal magnetic field and two horizontal electric field variations) measurements were made at each sounding locations using the wide-band MT data acquisition system (GMS 05) of M/s Metronix, Germany. The operational frequency range of GMS 05 is (4,096 s)$^{-1}$ to 8,192 Hz. The total frequency range of the system is split into five bands: (1) 256–8192 Hz; (2) 8–256 Hz; (3) 4^{-1}–8 Hz; (4) 128^{-1}–4^{-1} Hz; and (5) 4096^{-1}–128^{-1} Hz (by digital filtering of band 4). Also, the GMS 05 system enables the recording of a single band at a time. Electric dipoles of 80 m length with Cd-$CdCl_2$ electrodes were used to measure the two horizontal electric field variations (geomagnetic north-south (E_x) and east-west (E_y) components) and induction coils were used to record the three magnetic field (two horizontal—H_x (geomagnetic north-south) and H_y (geomagnetic east-west); and one vertical—H_z) components). The recording in the 10^{-1}–10^{1} Hz (Band 3) range started at 8:14 IST (2:44:00 UT) and continued till 9:39 IST (4:09:00 UT) with 32 Hz sampling rate. The Bhuj earthquake (origin time 3:16:40.7 UT) occurred during this recording. In this paper, we present the analysis of the MT data measured during this period. For convenience, we define 1024 data samples as a 'stack'. The total volume of data recorded is 160×1024 (i.e. 160 stacks) in each of the five channels. This data set form the basis of the analysis described in this paper.

The amplitude of natural EM signal in the frequency

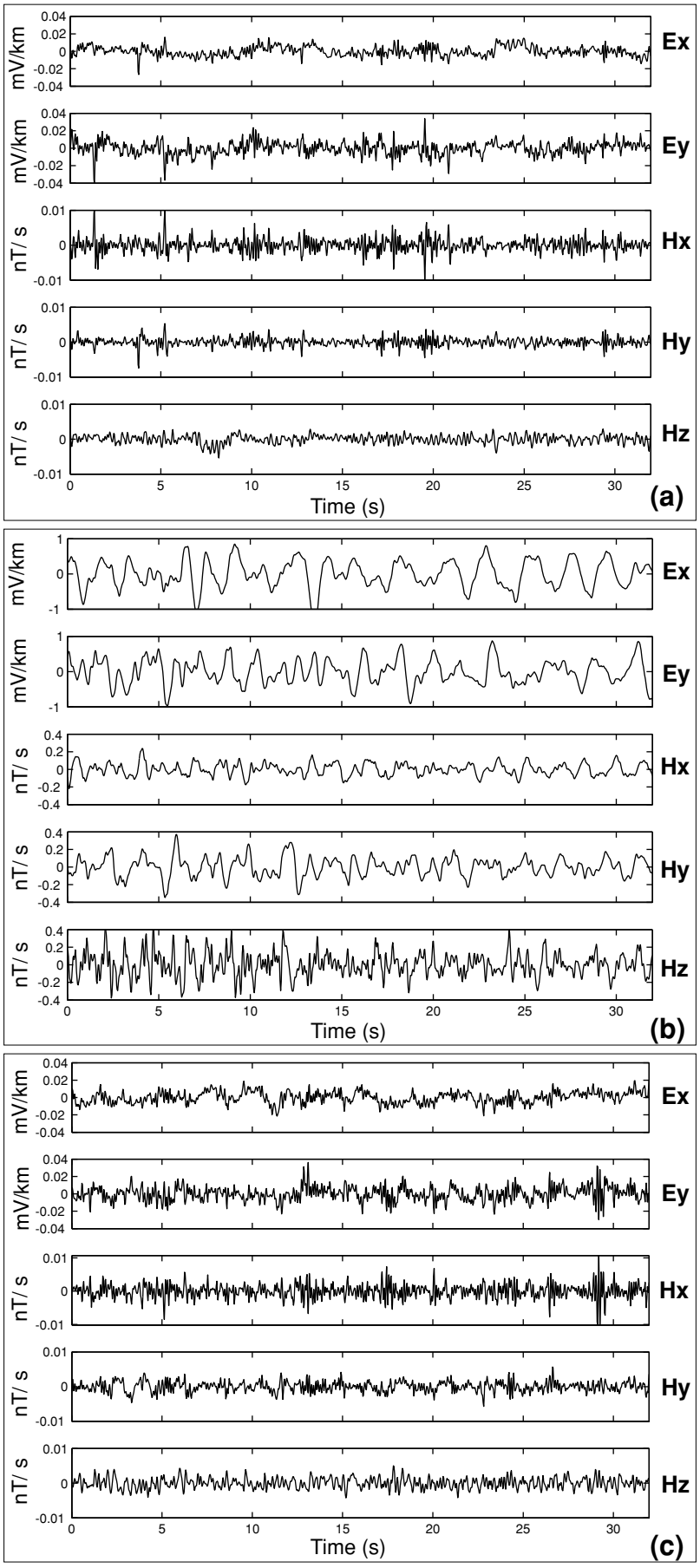

Fig. 3. Closer look at three segments of the time series data presented in Fig. 2, (a), during (b) and after (c) the Bhuj earthquake. Note the increase in signal amplitude during the earthquake (b). Low frequency signals dominate during the earthquake.

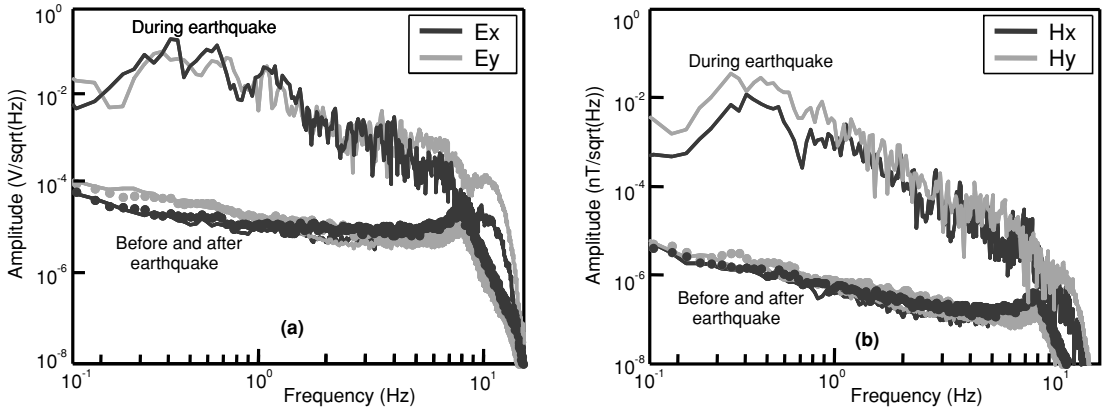

Fig. 4. Computed amplitude spectra for the electric field (a) and magnetic field (b), are shown for the signals recorded before, after and during the earthquake. Typical flat natural spectrum is observed before and after the earthquake. Large increase in spectral amplitudes is visible during the earthquake.

range 10^{-1}–10^{1} Hz rarely exceeds 0.050 mV/km for electric components and 0.020 nT for magnetic components; and look random in nature. This is because the natural EM waves have least energy in this period range (Simpson and Bahr, 2005). Figure 2 present the complete record of the time series. It clearly shows the increase in signal amplitudes, both in the electric and magnetic components, near 3:18:10 UT. The high amplitude signals last nearly 200 seconds. The time series in all the five channels shows that these high amplitude signals start soon after the earthquake origin time (EOT) with an approximate time delay of 100 s. The figure also shows a few high amplitude spikes in the electric and magnetic fields after the earthquake. In addition, it is also evident from the figure that (1) change in signal amplitude is more in electric channels (2) Hz is more affected among the magnetic signals, and (3) maximum electric field amplitude reaches up to ± 1.5 mV/km and magnetic field amplitude reaches up to ± 1 nT.

A close look of the time series, as presented in Fig. 3, shows three segments (each with 1024 data points) of the data set representing EM signals prior (Fig. 3(a)), during (Fig. 3(b)) and after (Fig. 3(c)) the seismic event. The time series prior and after the earthquake event show similar variations, and is within the normal amplitude range observed for this frequency range. In contrast, the MT signals recorded during the seismic event (Fig. 3(b)) show distinct changes in signal amplitude and sinusoidal fluctuations dominates the five components. These co-seismic signals begin about 100 s after the main shock. It can also be observed that the electric fields during the earthquake are not showing similar behavior. This may support the argument that the anomalous behavior in the electric field is not merely due to vibration of the electric field sensors and cables. The amplitudes of the electric field components reaches up to ± 1 mV/km; while the magnetic components reaches up to ± 0.5 nT, during the seismic activity.

3. Spectral Characteristics of the MT Time Series

We present the amplitude spectra of the electric and magnetic fields from segments of time series before; during and after the earthquake (Fig. 4). We removed the whole data windows affected by spikes. A spike is defined maximum 3 adjacent data points with large amplitudes as compared a 100 point running mean. The amplitude spectra show the typical flat natural spectrum, usually observed in MT signals in the frequency range 0.1 Hz to 10 Hz, before and after the earthquake in electric as well as in magnetic field data. The signals during the earthquake show a drastic change in spectral amplitudes of two electric field components and magnetic fields. The electric field show two orders higher spectral amplitude values for the signals during the earthquake, as compared to the signals observed prior and after the event (Fig. 4(a)). The magnetic spectra, on the other hand, shows three times increase during the earthquake signal (Fig. 4(b)). The amplitude spectra of the field components measured during the earthquake peaks around 0.4 Hz (2.5 s). However, the FFT based analysis is not suitable to bring out the temporal changes in frequency content of the signal.

4. Wavelet Analysis of the Data

Wavelet transform (c.f. Kumar and Foufoula-Georgiou, 1997) is a powerful tool to analyze the time series data with temporal variations in frequency. Wavelet analysis can reveal the characteristic of a signal as a function of time and frequency hence is superior to Fourier analysis (Lin *et al.*, 2002). The Continuous Wavelet Transform (CWT) of a

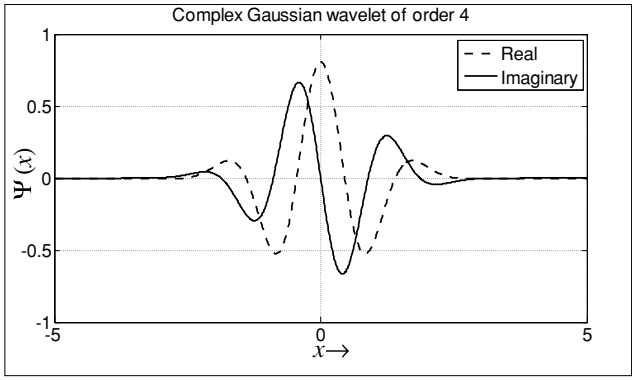

Fig. 5. The Gaussian mother wavelet used for the wavelet analysis of magnetotelluric time series.

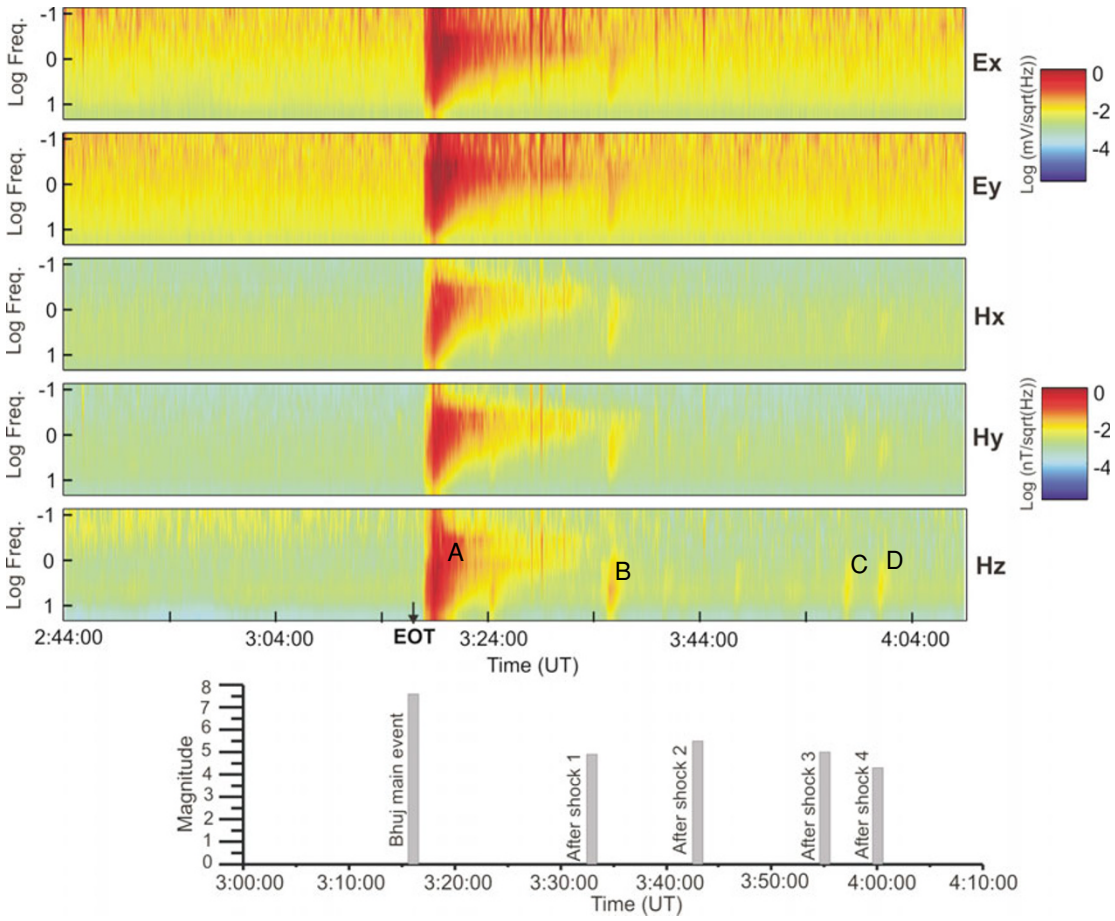

Fig. 6. Wavelet power spectral plot for the five MT channels. The alphabets A, B, C and D represents the different spectral regimes present in the wavelet spectrum. The occurrence of Bhuj earthquake aftershocks are also compared with the different spectral regimes observed in the wavelet spectra.

signal $x(t)$ is defined as:

$$X_\omega(a,b) = \frac{1}{\sqrt{|a|}} \int_{-\infty}^{\infty} x(t)\ \psi\left(\frac{t-b}{a}\right) dt,$$

where a is called dilation parameter (scale lengths) which controls the frequency of the wavelet and b is the translation parameter which controls the movement of the wavelet along the time axis. The function ψ denotes the mother wavelet. We use fourth order Gaussian mother wavelets for the analysis. It is defined as, $\psi(x) = C_n \frac{d^n}{dx^n} e^{-i\omega x} e^{-x^2}$ (where $n = 4$). Here C_n is a constant to normalize the function ψ so that it has unit energy. Gaussian wavelet gives the most accurate estimation of frequency components localized in time (Cohen and Kovacevic, 1996). The Gaussian mother wavelet is plotted in Fig. 5.

We obtained wavelet power spectral estimates using scale lengths (a) 160 to 1, corresponding to the frequency range 0.1–16 Hz. Plots of the wavelet spectra, for the entire records of electric and magnetic channels are shown in Fig. 6. The wavelet spectra clearly show two distinct spectral regimes for the MT signals. The signals observed before the onset of the main shock shows the natural MT flat spectrum. The sharp rise in the spectral amplitudes, across all the frequency range, starting around 3: 18:10 UT (marked A) marks the signal related to the earthquake. This is observed both in electric and magnetic channels. With the progress of time, the energy gets limited to the frequency band 2–0.4 Hz. The extension of these co-seismic signals is seen up to 3:32 UT. The presence of three more events of similar spectral characteristics (marked as B, C and D in Fig. 6) occurring after the main shock is also notable. This is more evident in the vertical magnetic field (H_z) channel. The B region, near 3:35 UT, has clearly signal energy spread throughout the frequency range whereas in the C and D regions the signal is limited to a narrow band (2–10 Hz). The Bhuj area recorded many after shock events and the after shock events occurred during the recording period of our data set are shown in the bottom panel of the Fig. 6. It is seen that the majority of the aftershock activities show correlation with the enhanced spectra (B, C and D) in the wavelet spectrum. Hence, it can be speculated that the enhanced spectra (segments B, C, and D) observed are associated with the after shock events. However, the second after shock event (3:43 UT) did not produce any clear EM signatures in the data and we are unable to explain this observation. It may be concluded that wavelet analysis has brought out temporal as well as frequency variations in the EM signals related to earthquake. In addition, the weak signals, probably related to the aftershock events, also could be seen in the wavelet spectrum.

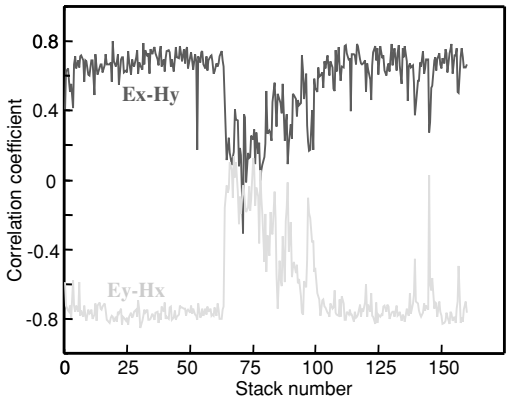

Fig. 7. The correlation coefficients obtained between the orthogonal fields, E_x-H_y and E_y-H_x are plotted against the stack numbers (one stack equals 32 s of MT data or 1024 data samples). Significant drop in correlation coefficient values is seen between stacks 65 and 100.

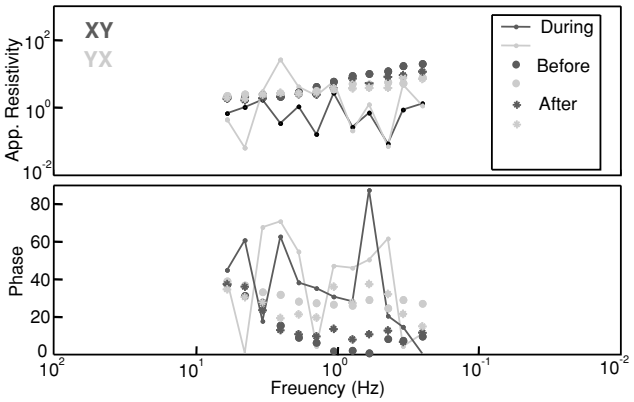

Fig. 8. Magnetotellluric impedance (shown as apparent resistivity and phase) estimated from time series segments recorded before (filled circles), during (solid line) and after (stars) the earthquake.

5. MT Impedances

The simultaneous measurement of the five component MT signals facilitates the calculation of MT impedance values. The MT apparent resistivity and phase estimates from the time series segment measured during the earthquake event is compared with the estimates made from time series not affected with the co-seismic signal (Fig. 7). We did not use any noise elimination procedures for processing the data. The MT impedance values, shown as apparent resistivity and phase data, computed using the data during the earthquake are scattered. The MT parameters (apparent resistivity and phase) estimated before and after the event shows no major differences between them and indicate smoother curves suggesting that the during the pre and post earthquake period, the electric and magnetic fields were related through an MT transfer function. However, this relation breaks down during the earthquake.

We have also studied the Pearson's correlation coefficients (Molyneux and Schmitt, 1999) between the observed electric and magnetic fields. Pearson's correlation reflects the degree of linear relationship between two variables. It is calculated as,

$$r = \frac{\sum_{i=1}^{n} \left(X_i - \overline{X}\right)\left(Y_i - \overline{Y}\right)}{(n-1)S_x S_y}$$

where, $\overline{X}$ and $\overline{Y}$ indicate the means of the variable X and Y, and S_x and S_y are their standard deviations. It ranges from $+1$ to -1. A correlation value of $+1$ means a perfect positive linear relationship between the variables.

The correlation coefficients between the orthogonal electric and magnetic fields (i.e., E_x-H_y and E_y-H_x) show drastic drop in correlation for the data measured during earthquake, while the MT fields are well correlated before and after the earthquake as indicated by high correlation coefficient (Fig. 8). Hence, the much poor impedance estimation during the earthquake indicates that the high amplitude signals are not related to each other by MT transfer function. This strengthens the argument that the high amplitude electric and magnetic signals present during the earthquake are not natural MT signals.

6. Discussion on the Observed Co-seismic Phenomena

The MT mid frequency range (10^{-1}–10^{1} Hz) signals recorded ~350 km away from the epicenter region of Bhuj earthquake clearly describes the existence of co-seismic EM events in all the telluric and magnetic measurements. The spectral analysis and wavelet analysis of the data show anomalous electric and magnetic signals during the earthquake time. The MT impedance values and the correlation coefficients between the orthogonal electric and magnetic fields suggest that the MT time series recorded during the earthquake are not related to each other through a transfer function.

Egbert and Booker (1986) discuss the effect of geomagnetic storms that can give rise to high amplitude signals in MT recording as observed in our case and can contaminate the MT data resulting in a poor MT transfer functions estimation. To make sure that the observed anomalous signals during the earthquake as co-seismic EM signals, we looked for external disturbances of magnetospheric origin for these signals. The planetary index for the geomagnetic activity level (K_p index) had a value of 2 (indicating rather quiet geomagnetic activity) for the three hours preceding the Bhuj event. In addition, the closest geomagnetic observatory at Alibagh, about 325 km south to our MT observation site (~600 km south-east from epicenter), does not show any anomalous signals during the Bhuj earthquake. Hence the possibility of external origin for the anomalous MT signals can be eliminated and the observed variations in the electric and magnetic field during the earthquake could be associated with the seismic activity. Such co-seismic electric and magnetic signals have been observed during many earthquakes (e.g. Honkura *et al.*, 2000; Nagao *et al.*, 2000; Karakelian *et al.*, 2002; Matsushima *et al.*, 2002; Zlotnicki *et al.*, 2006) and our results corroborates with it.

The phenomena of electric and magnetic signals associated with seismic activity have been previously reported and analyzed (e.g. Hayakawa *et al.*, 1996; Honkura *et al.*, 2000; Nagao *et al.*, 2000, 2002; Enomoto *et al.*, 2006; Hattori *et al.*, 2006; Zlotnicki *et al.*, 2006). These EM signals, observed well before and during (co-seismic) an earthquake, spread over ULF, ELF and VLF frequency ranges. The

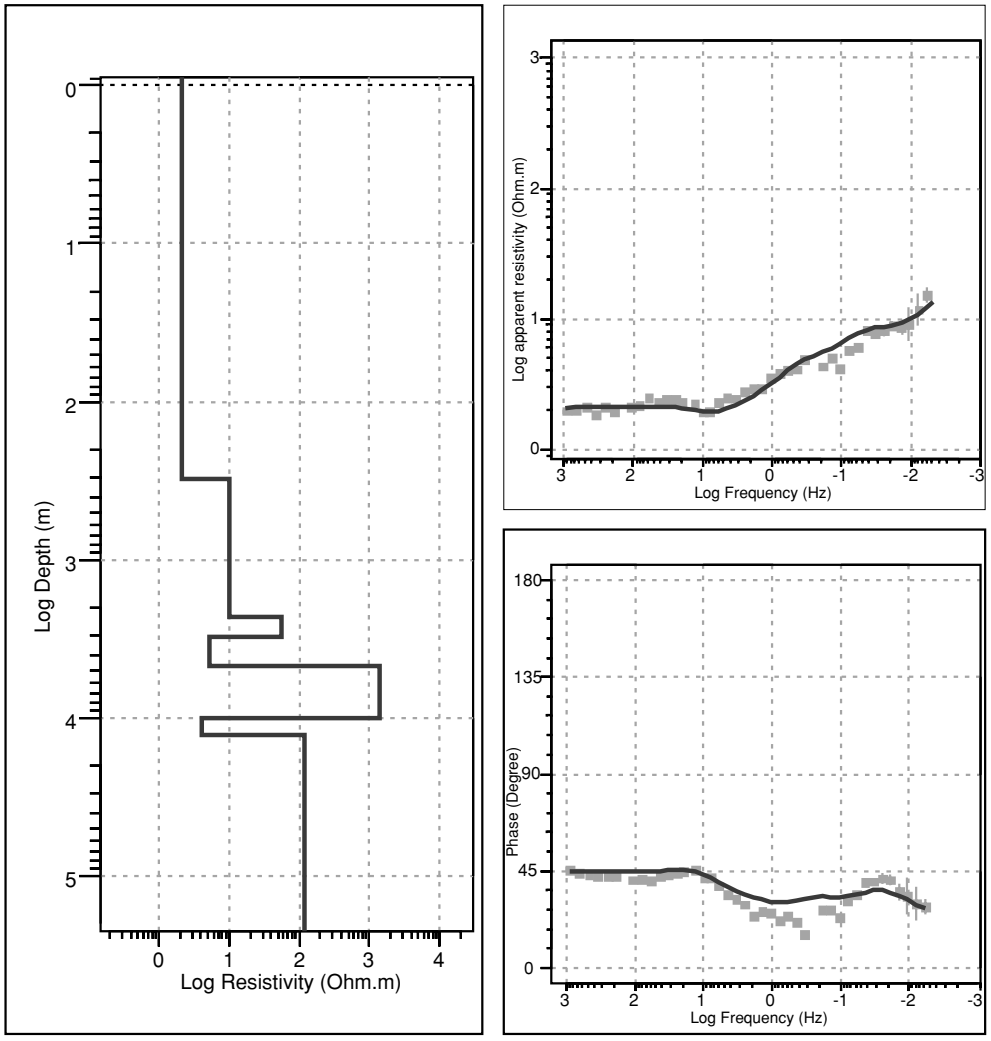

Fig. 9. Layered electric model (left) obtained from the determinant impedance data using Marquardt (1963) inversion approach. Measured (symbols) and model response (solid line) apparent resistivity and phase are illustrated in the right.

case studies have shown co-seismic ULF (10^{1}–10^{-2} Hz) signals recorded at distance of ∼150 km from the epicenter (Zlotnicki *et al*., 2006). In the present study, co-seismic EM signals are recorded on all the components of the electric and magnetic fields, and they appear ∼100 s after the earthquake origin time. It is unlikely that these anomalous co-seismic signals being electromagnetic impulses radiated from the earthquake source, since the EM signals get diffused within few kilometers (Fujinawa *et al*., 2001). The study region, encompassing our observation site and the earthquake location, is characterized by major Mesozoic rift zones (i.e. Narmada and Cambay rift zone) and several major neotectonic faults (Fig. 1). Mesozoic sediments were uplifted, folded, intruded and covered by Deccan Trap basaltic flows in Late Cretaceous and early Paleocene time (Biswas, 1987). Thick sediment formations ranging in age from Middle Jurassic to present are also inferred in these rift zones. The study of seismic wave velocities in the Bhuj earthquake area have shown fractured rock matrix with fluids in the hypocentral region (23–28 km) and suggested a fluid driven earthquake similar to 1995 Kobe earthquake (Mishra and Zhao, 2003) which also observed co-seismic electromagnetic changes (Nagao *et al*., 2002). Magnetotelluric studies in this region delineated major electrically conductive regions in the crust (Gokarn *et al*., 2001; Patro *et al*., 2005; Sastry *et al*., 2008). The conductive crust will not allow the EM signals (10^{-1}–10^{1} Hz) to travel from earthquake epicenter to MT observation site located at ∼350 km. Hence it is reasonable to conclude that the anomalous high amplitude EM signals recorded are not the direct radiations from the earthquake source and are generated in the vicinity of the station with the arrival of seismic waves (e.g. Nagao *et al*., 2000; Karakelian *et al*., 2002).

Various mechanisms are proposed for the generation of the anomalous EM fields associated with the earthquake process (Johnston, 1997; Ogawa and Utada, 2000; Guglielmi *et al*., 2004). Most of these are based on the drastic stress changes associated with the earthquake process and the resulting crustal phenomena. Prominent generation mechanisms proposed to explain the co-seismic EM signals are based on electrokinetic effect (Zlotnicki and Le Mouel, 1990; Fenoglio *et al*., 1995; Nagao *et al*., 2000) and seismic dynamo effect (Honkura *et al*., 2000, 2002).

The MT sounding data obtained at the observation site is analyzed and modeled to understand the subsurface resistivity structure. One-dimensional geo-electric model is

derived by inverting the invariant determinant impedance values (Ranganayaki, 1984) in the 10^{-3}–500 s range, using Marquardt (1963) approach. Figure 9 shows the layered resistivity model and the model response fit with the observed impedance values. The model shows a conductive (2–10 Ohm.m) layers on the top with about 2.3 km thickness. A relatively resistive (55 Ohm.m) layer having ~800 m thickness underlies the top conductive layers. Another 5 Ohm.m conductive layer is present below the above resistive layer and shows a thickness of 1.6 km. This conductive layer sits on a high resistive (1400 Ohm.m) formation of about 5.2 km thickness. Underneath this high resistive layer, high conductive layer is modeled. However, this deeper part of model is not highly sensitive to the data and hence not well resolved. The top conductive layers observed in the model represent the thick tertiary formations in the area. The moderately resistive layer could be the image of fractured basaltic layer covering the area. The conductive formations underneath this basaltic layer can be interpreted as the Mesozoic sedimentary formations. The high resistive gneissic basement rocks underlie this Mesozoic formation. This model is well correlated with the known geology of the region (Biswas, 1987). The region is well known for its hydrocarbon resources and many producing wells are located in the Cambay basin (Negi *et al*., 2006). Drilled boreholes in the regions have shown tertiary sediment thicknesses up to 2.5 km. In short, the MT model also shows thick tertiary sediments and trap covered Mesozoic formations at the observation site. The presence of fractured, fluid filled tectonic structures in the vicinity of the MT site and sedimentary formations under the observation site are favorable conditions to produce co-seismic electromagnetic signals by electro-kinetic mechanism.

Co-seismic electric and magnetic fields can be generated by seismic dynamo effect associated with the passage of seismic waves (Honkura *et al*., 2002). Seismic dynamo effect is the EM induction in the conducting earth caused by ground vibration in the static magnetic field of the earth. Such a mechanism has been projected for the anomalous co-seismic EM signals observed during earthquakes (Honkura *et al*., 2000, 2002, 2004; Matsushima *et al*., 2002; Ujihara *et al*., 2004). EM field generation is also possible due to the vibration of the cables and sensors during the passage of seismic waves. Experimental studies made by Ujihara *et al*. (2004) and Mogi *et al*. (2000) have shown that the co-seismic EM cannot be fully accounted for by the shaking effect of cables and sensors. We therefore prefer to exclude the possibility of co-seismic EM changes caused merely due to the vibration of connecting cables and sensors in the Earth's magnetic field. Similar opinion is made by Nagao *et al*. (2000) who analyzed the co-seismic electric field variations observed in Japan.

It is difficult to attribute a single mechanism for the cause of co-seismic EM signals observed in the MT records. However, the results confirm the fact that electromagnetic fields are generated in the subsurface during the passage of seismic wave. The apparent resistivity and phase values calculated shows that the measured MT parameters prior and after the main event are similar and suggest that no substantial subsurface conductivity changes at the observation point due to the seismic activity. The correlation between the prominent wavelet signatures and the aftershock activity suggest that EM field variations can be produced at long distance by aftershock events.

7. Conclusions

We present the analysis of the electric and magnetic fields measured during the high magnitude (M_w 7.6) Bhuj earthquake of 26 January 2001. The analysis brought out the time-frequency characteristics of the anomalous EM signals observed both in electric and magnetic field during the earthquake. The spectral amplitude of the electric fields show two orders higher than the signals observed prior and after the event; while magnetic fields show three times increase in spectral power. The wavelet analysis brought out the time-frequency characteristics of the electromagnetic signals related to the seismic activity. The existence of signals with similar frequency characteristics, probably related to the weaker after shock events, was also brought by wavelet spectra. It is also seen that the anomalous electric and magnetic fields are not related to each other through an MT transfer function in contrast to the signals recorded prior and after the earthquake. Absence of any geomagnetic storm activity during the earthquake time excludes the possibility of external origin for the anomalous EM signals. The geological and tectonic elements in the region suggest favorable conditions for the generation of co-seismic EM signals due to electro-kinetic effects and seismic dynamo effect by the seismic waves. We would like to conclude that both electro-kinetic and seismic dynamo effects could be the generation mechanisms for the observed co-seismic electromagnetic field variations in the study.

Acknowledgments. We thank director, NGRI, for his kind permission to publish this work. We appreciate the constructive comments by Dr. Zlotnciki and an anonymous reviewer.

References

Biswas, S. K., Regional tectonic framework, structure and evolution of the western marginal basins of India, *Tectonophysics*, **135**, 307–327, 1987.

Cohen, A. and J. Kovacevic, Wavelets: the mathematical background, *Proc. IEEE*, **84**(4), 1996.

Egbert, G. and J. R. Booker, Robust estimation of geomagnetic transfer functions, *Geophys. J. Int*., **87**, 173–194, 1986.

Enomoto, Y., H. Hashimoto, N. Shirai, Y. Murakami, T. Mogi, M. Takada, and M. Kasahara, Anomalous geoelectric signals possibly related to the 200 Mt. Usu eruption and 2003 Tokachi-Oki earthquakes, *Phys. Chem. Earth*, **31**, 319–324, 2006.

Fenoglio, M. A., M. J. S. Johnston, and J. Byerlee, Magnetic and electric fields associated with changes in high pore pressure in fault zones—Application to the Loma Prieta ULF emissions, *J. Geophys. Res*., **100**, 12951–12958, 1995.

Fujinawa, Y., K. Takahashi, T. Matsumoto, H. Iitala, T. Doi, T. Nakayama, T. Sawada, and H. Sakai, Electric field variations related to seismic swarms, *Bull. Earthq. Res. Inst. Univ. Tokyo*, **76**, 391–415, 2001.

Gokarn, S. G., C. K. Rao, G. Gupta, B. P. Singh, and M. Yamashita, Deep crustal structure in central India using magnetotelluric studies, *Geophys. J. Int*., **144**, 685–694, 2001.

GSI, Seismotectonic atlas of India and its environs, Geological Survey of India, 2000.

Guglielmi, A., A. Potapov, and B. Tsegmed, One mechanism for generation of the co-seismic electromagnetic oscillations, *Phys. Chem. Earth*, **29**, 453–457, 2004.

Harinarayana and others, Exploration of sub-trappean Mesozoic basins in the western part of Narmada-Tapti region of Deccan Syneclise, *NGRI Tech. Report (unpublished), National Geophys. Res. Inst., Hyderabad,*

India, No: NGRI-2003-EXP-404, 2004.

Hattori, K., A. Serita, C. Yoshino, M. Hayakawa, and N. Isezaki, Singular spectral analysis and principal component analysis for signal discrimination of ULF geomagnetic data associated with 2000 Izu Island Earthquake Swarm, *Phys. Chem. Earth*, **31**, 281–291, 2006.

Hayakawa, M., R. Kawate, O. A. Molchanov, and K. Yumoto, Results of ultra-low-frequency magnetic field measurements during the Guam earthquake of 8 August 1993, *Geophys. Res. Lett.*, **23**, 241–244, 1996.

Honkura, Y., A. M. Isikira, N. Oshiman, A. Ito, B. Ucer, S. Baris, M. K. Tuncer, M. Matsushima, R. Pektas, C. Celik, S. B. Tank, F. Takahashi, M. Nakanishi, R. Yoshimura, Y. Ikeda, and T. Komut, Preliminary results of multidisciplinary observations before, during and after the Kocaeli (Izmit) earthquake in the western part of the North Anatolian Fault Zone, *Earth Planets Space*, **52**, 293–298, 2000.

Honkura, Y., M. Matsushima, N. Oshiman, M. K. Tuncer, S. Baris, A. Ito, Y. Iio, and A. M. Isikara, Small electric and magnetic signals observed before the arrival of seismic wave, *Earth Planets Space*, **54**, e9–e12, 2002.

Honkura, Y., H. Satoh, and N. Ujihara, Seismo dynamo effects associated with the M7.1 earthquake of 26 May 2003 off Miyagi Prefecture and the M6.4 earthquake of 26 July 2003 in northern Miyagi Prefecture, NE Japan, *Earth Planets Space*, **56**, 109–114, 2004.

Johnston, M. J. S., Review of electric and magnetic fields accompanying seismic and volcanic activity, *Surv. Geophys.*, **18**, 441–475, 1997.

Karakelian, D., S. L. Klemperer, A. C. Fraser-Smith, and G. A. Thompson, Ultra-low frequency electromagnetic measurements associated with the 1998 Mw 5.1 San Juan Bautista, California earthquake and implications for mechanisms of electromagnetic earthquake precursors, *Tectonophysics*, **359**, 65–79, 2002.

Kumar, P. and E. Foufoula-Georgiou, Wavelet Applications in Geophysics: A Review, *Rev. Geophys.*, **35**, 385–412, 1997.

Lin, Y., Q. Li, M. Hayakawa, and X. Zeng, Wavelet analysis and seismomagnetic effect, in *Seismo Electromagnetics: Lithosphere Atmosphere Ionosphere Coupling*, edited by Hayakawa and Molchanov, 61–68, TERRAPUB, Tokyo, 2002.

Marquardt, D. W., An algorithm for least-square estimation of non-linear parameters, *J. SIMA*, **11**, 431–441, 1963.

Matsushima, M. and others, Seismoelectromagnetic Effect Associated with the İzmit Earthquake, *Bull. Seismol. Soc. Am.*, **92**, 350–360, 2002.

Mishra, O. P. and D. Zhao, Crack density, saturation rate and porosity at the 2001 Bhuj, India, earthquake hypocenter: a fluid-driven earthquake?, *Earth Planet. Sci. Lett.*, **212**, 393–405, 2003.

Mogi, T., Y. Tanaka, D. S. Widarto, E. M. Arsadi, N. T. Puspito, T. Nagao, W. Kanda, and S. Uyeda, Geoelectric potential difference monitoring in southern Simatra, Indonesia,—Co-seismic change, *Earth Planets Space*, **52**, 245–252, 2000.

Molyneux, J. B. and D. R. Schmitt, First-break timing: arrival onset times by direct correlation, *Geophysics*, **64**, 1492–1501, 1999.

Nagao, T., Y. Orihara, T. Yamaguchi, I. Takahashi, K. Hattori, Y. Noda, K. Sayanagi, and S. Uyeda, Co-seismic geoelectric potential change observed in Japan, *Geophys. Res. Lett.*, **27**(10), 1535–1538, 2000.

Nagao, T., Y. Enomoto, Y. Fujinawa, M. Hata, M. Hayakawa, Q. Huang, J. Izutsu, Y. Kushida, K. Maeda, K. Oike, S. Uyeda, and T. Yoshino, Electromagnetic anomalies associated with 1995 Kobe earthquake, *J. Geodyn.*, **33**, 401–411, 2002.

Negi, A. S., S. K. Sahu, P. D. Thomas, D. S. A. N. Raju, R. Chand, and J. Ram, Fusing geologic knowledge and seismic in searching for subtle hydrocarbon traps in India's Cambay Basin, *The Leading Edge*, **25**, 872–880, 2006.

Ogawa, T. and H. Utada, Electromgnetic signals related to incidence of a teleseismic body wave into a subsurface piezoelectric body, *Earth Planets Space*, **52**, 252–260, 2000.

Patro, B. P. K., T. Harinarayana, R. S. Sastry, M. Rao, C. Manoj, K. Naganjaneyulu, and S. V. S. Sarma, Electrical imaging of Narmada-Son Lineament Zone, Central India from magnetotellurics, *Phys. Earth Planet. Inter.*, **148**, 215–232, 2005.

Ranganayaki, R. P., An interpretive analysis of magnetotelluric data, *Geophysics*, **49**, 1730–1748, 1984.

Sastry, R. S., N. Nandini, and S. V. S. Sarma, Electrical imaging of deep crustal features of Kutch, India, *Geophys. J. Int.*, **172**, 934–944, 2008.

Simpson, F. and K. Bahr, *Practical Magnetotellurics*, Cambridge University Press, 2005.

Singh, V., B. Singh, M. Kumar, and M. Haykawa, Identification of earthquake sources responsible for subsurface VLF electric field emissions observed at Agra, *Phys. Chem. Earth*, **31**, 325–335, 2006.

Ujihara, N., Y. Honkura, and Y. Ogawa, Electric and magnetic field variations arising from the seismic dynamo effect for aftershocks of the M7.1 earthquake of 26 May 2003 off Miyagi Prefecture, NE Japan, *Earth Planets Space*, **56**, 115–123, 2004.

Widarto, D., T. Mogi, Y. Tanaka, T. Nagao, K. Hattori, and S. Uyeda, Co-seismic geoelectrical potential changes associated with the June 4, 2000's earthquake (Mw 7.9) in Bengkulu, Indonesia, *Phys. Chem. Earth*, **34**, 373–379, 2009.

Zlotnicki, J. and J. Le Mouel, Possible electrokinetic origin of large magnetic variations at la Fournaise volcano, *Nature*, **343**, 633–636, 1990.

Zlotnicki, J., V. Kossobokov, and J. Le Mouel, Frequency spectral properties of an ULF electromagnetic signal around the 21 July 1995, M=5.7, Yong Deng (China) earthquake, *Tectonophysics*, **334**, 259–270, 2001.

Zlotnicki, J., J. L. Le Mouel, R. Kanwar, P. Yvetot, G. Vargemezis, P. Menny, and F. Fauquet, Ground-based electromagnetic studies combined with remote sensing based on Demeter mission: A way to monitor active faults and volcanoes, *Planet. Space Sci.*, **54**, 541–557, 2006.

K. K. Abdul Azeez (e-mail: azeez@ngri.res.in), C. Manoj, K. Veeraswamy, and T. Harinarayana